320–326 Nucleic Acids Research, 1995, Vol. 23, No. 3

Interaction of the yeast splicing factor PRP8 with substrate RNA during both steps of splicing

Stefan Teigelkamp+, Erica Whittaker§ and Jean D. Beggs*

Institute of Cell and Molecular Biology, University of Edinburgh, King's Buildings, Mayfield Road, Edinburgh EH9 3JR, UK

Received December 5, 1994; Accepted December 30, 1994

ABSTRACT

PRP8 protein of *Saccharomyces cerevisiae* interacts directly with pre-mRNA in spliceosomes, shown previously by UV-crosslinking. To analyse at which steps of splicing and with which precursor-derived RNA species the interaction(s) take place, UV-crosslinking was combined with PRP8-specific immunoprecipitation and the coprecipitated RNA species were analysed. Specific precipitation of intron–exon 2 and excised intron species was observed. PRP8 protein could be UV-crosslinked to pre-mRNA in PRP2-depleted spliceosomes stalled before initiation of the splicing reaction. Thus, the interaction of PRP8 protein with substrate RNA is established prior to the first transesterification reaction, is maintained during both steps of splicing and continues with the excised intron after completion of the splicing reaction. RNase T1 treatment of spliceosomes revealed that substrate RNA fragments of the 5′ splice site region and the branchpoint-3′ splice site region could be coimmunoprecipitated with PRP8 specific antibodies, indicating that these are potential sites of interaction for PRP8 protein with substrate RNA. Protection of the branchpoint-3′ splice site region was detected only after step 1 of splicing. The results allow a first glimpse at the pattern of PRP8 protein–RNA interactions during splicing and provide a fundamental basis for future analysis of these interactions.

INTRODUCTION

Nuclear pre-mRNA splicing takes place in a large ribonucleoprotein complex, the spliceosome. Four small nuclear ribonucleoprotein particles (snRNPs) containing the U1, U2, U4, U5 and U6 small nuclear RNAs (snRNAs) and a number of snRNP-proteins assemble in precisely defined consecutive steps to form a functional spliceosome. Additional non-snRNP proteins including some transiently interacting protein factors are required for splicing activity (for review, see 1,2). The first step in spliceosome assembly is the association of the U1 snRNP with the 5′ splice site region of the pre-mRNA, followed by the ATP-dependent association of the U2 snRNP with the branchpoint region. The U4/U6 snRNP interacts with the U5 snRNP to form the U4/U6.U5 triple snRNP which then associates with the U1–U2–pre-mRNA complex to form the spliceosome. The U4/U6 interaction is disrupted to allow association of U6 snRNA with U2 snRNA and with the intron near the 5′ splice site in the spliceosome (for review, see 3) and the U5 snRNA associates with exon nucleotides at the 5′ splice site (3–5). Subsequently, the intron is removed in two transesterification reactions. The U5 snRNA interacts with exon nucleotides at the 3′ splice site prior to the second transesterification step, thereby aligning the two exons for ligation (5,6). Various steps during spliceosome assembly and processing utilize ATP.

In addition to an snRNA, each snRNP contains a set of common snRNP proteins and proteins specific to the individual snRNP (for review, see 7–9). A number of these proteins have been identified in HeLa cells and in *Saccharomyces cerevisiae*. In contrast to the human proteins, which were characterized biochemically, the majority of the splicing factors in *S.cerevisiae* has been identified through genetic screening of *prp*-mutants (pre-mRNA processing) having defects in pre-mRNA splicing.

The gene encoding the PRP8 protein, the subject of this work, was cloned by complementation of the temperature-sensitive mutation *prp8-1* (previously called *rna8-1*; 10). It encodes an unusually large protein of 280 kDa. A *prp8* allele has been isolated as a genetic suppressor of the DEAD-box protein splicing factor *PRP28*, a putative RNA helicase. From this a model was proposed in which PRP28 protein destabilizes the U4/U6 snRNA interaction prior to step 1 of splicing, counterbalanced by a stabilizing effect of PRP8 protein (11). A mutation affecting another DEAD-box protein, DED1, has been isolated as a cold-sensitive suppressor of a temperature-sensitive *prp8* allele (12). Thus, PRP8 protein might be responsible for the stability of RNA–RNA interactions in the spliceosome.

Antibodies raised against the yeast PRP8 protein detect homologues in all species investigated, such as humans (13),

* To whom correspondence should be addressed

Present addresses: +Institute für Molekularbiologie und Tumorforschung, Philipps-Universität Marburg, Emil-Mannkopff-Strasse 2, 35037 Marburg, Germany and §PPL Therapeutics, Roslin, Edinburgh EH25 9PP, UK

mouse (P. Hodges and J. D. B., unpublished), *Drosophila* (14) and higher plants (15). Since the high molecular weight (>200 kDa) appears to be conserved among all homologues, the large size might be essential for the function of PRP8 protein. The primary sequence shows an extraordinarily high degree of conservation among species (16) with no obvious homology to other proteins, suggesting a critical role for PRP8 in the splicing process. The most striking feature of the yeast protein is an acidic N-terminus containing four proline$_{(4-8)}$ repeats; however, this motif may not be conserved in the related *C.elegans* protein (16). Biochemical studies revealed that PRP8 protein is a stable component of the U5 snRNP and an intrinsic component of spliceosomes (17,18). Similar results have been obtained for p220, the human homologue of PRP8 (19). *In vitro*, PRP8 protein appears to play a role in formation of U4/U6.U5 tri-snRNP complexes and in the assembly of triple snRNPs into forming spliceosomes. Furthermore, *in vivo* depletion of PRP8 protein results in degradation of U4, U5 and U6 snRNAs (20). Following incorporation of the U4/U6.U5 triple snRNP into spliceosomes, PRP8 protein as well as the human p220 homologue interact directly with the pre-mRNA substrate, shown by UV-crosslinking (21,22). We demonstrate here that this interaction is established prior to step 1 of splicing, is maintained during splicing and continues after step 2 is complete. RNAse T1 protection assays indicate that the 5′ splice site region and the branchpoint-3′ splice site region are potential binding sites for PRP8 protein.

MATERIALS AND METHODS

Yeast strains, plasmids and RNA substrates

S.cerevisiae strains BJ2412 and SPJ8.31 were described previously (12,17) and DJY85 (MAT**a**/α, *prp2-1/prp2-1, ura3/ura3, ade1/ADE1, ade2/ade2, trp1/TRP1, his3/HIS3, tyr1/TYR1, lys2-801/LYS2-801, can1/CAN1*) was obtained from D. J. Jamieson, Dundee.

The following plasmid DNAs were linearised by digestion with *Eco*RI to provide templates for *in vitro* transcription. Plasmid pT7rp28 (22) was transcribed *in vitro* with T7 RNA polymerase, and plasmid pSPrp51A (23) was transcribed *in vitro* with SP6 RNA polymerase to generate pre-mRNAs. The transcripts were uniformly ^{32}P-labelled by using 60 μCi [α-^{32}P]UTP (800 Ci/mmol, Amersham, UK) in a transcription reaction (18 μl) containing 8 μM UTP, according to the protocol of the manufacturer (Pharmacia LKB).

Splicing extract preparation and *in vitro* splicing reactions

Preparation of yeast whole cell extracts and *in vitro* splicing reactions were performed as described (24). Extracts from strain DJY85 were heat-inactivated as spheroplasts *in vivo* during extract preparation by incubation at 36°C for 1 h, followed by inactivation *in vitro* at 31°C for 15–30 min. PRP2Δ spliceosomes were assembled at 25°C for 20 min in a total volume of 50 μl containing 50% (v/v) heat-inactivated splicing extract from DJY85 cells, 0.2 pmol ^{32}P-labelled pre-mRNA, 1.5 mM ATP and 50% (v/v) splicing buffer (24). For complementation, PRP2Δ spliceosomes were mixed in a 1:1 ratio with a heat-inactivated (31°C, 1.5 h) splicing extract from strain SPJ8.31 and incubated at 25°C for 15 min. The reaction products were fractionated on 6% (w/v) polyacrylamide–8 M urea gels and visualised by autoradiography.

UV-crosslinking assay and immunoprecipitations

UV-light induced crosslinking of RNA to protein was performed essentially as described (22) in 50 μl aliquots, except that UV-irradiation was for 25 min on ice. Samples were subjected to denaturation by addition of SDS to 1% (w/v), Triton X-100 to 1% (v/v) and DTT to 100 mM and heated to 90°C for 1.5 min. To reduce the concentration of denaturants before immunoprecipitation, these samples were diluted 10-fold with immunoprecipitation buffer, containing 150 mM NaCl, 2.5 mM $MgCl_2$, 6 mM HEPES (pH 7.5), 0.05 % (v/v) NP-40, and protease inhibitors PMSF (200 μg/ml), Bestatin (40 μg/ml), Pepstatin (1.4 μg/ml) and Leupeptin (1 μg/ml).

Antiserum to PRP8–β-galactosidase fusion protein 8.4 has been described (17). Anti-8.6 antiserum was raised against a 35 amino acids N-terminal synthetic peptide of PRP8 protein (G. J. Anderson and J. D. B., unpublished). Antibodies were bound to protein A–Sepharose beads (PAS; Sigma) in TBSN buffer [145 mM NaCl, 50 mM Tris–HCl (pH 7.6), 0.05% (v/v) NP-40] and washed four times with the same buffer. UV-irradiated splicing reactions were incubated at 4°C with PAS-bound antibodies for 2 h with rotation. The antibody complexes were washed twice with TBSN and once with TBS (TBSN without NP-40). For analysis of substrate RNA species crosslinked to PRP8 protein, the washed PAS-bound complexes were treated with proteinase K for 45 min at 37°C in a total volume of 80 μl containing 300 mM NaCl, 50 mM Tris–HCl (pH 7.5), 5 mM EDTA, 1.5% (w/v) SDS and 2 mg/ml proteinase K (Boehringer Mannheim, UK), followed by extraction with phenol/chloroform and precipitation with ethanol. The reaction products were fractionated on 6% (w/v) polyacrylamide–8 M urea gels and visualised by autoradiography. For analysis of crosslinked PRP8 protein, samples were UV-irradiated, digested with RNAse T1 (5 U/μl final concentration, Boehringer Mannheim, UK) prior to immunoprecipitation, diluted with immunoprecipitation buffer to a final volume of 200 μl and immunoprecipitated as described above. Subsequently, immunoprecipitates were subjected to SDS–gel electrophoresis through 6% polyacrylamide gels. Gels were analysed by autoradiography.

Ribonuclease T1 protection assay

Standard splicing reactions of 50 μl were stopped on ice and *E.coli* tRNA was added to a final concentration of 0.2 mg/ml. Ribonuclease T1 was added to 2.5 U/μl, followed by incubation of the samples at 37°C for 30 min. Immunoprecipitations were performed as described above using either 8.4 or 8.6 antibodies. The protected RNA fragments were extracted with phenol, precipitated with ethanol, separated by electrophoresis on a denaturing 20% polyacrylamide gel and visualized by autoradiography. The RNA fragments were eluted from the gel and re-digested with RNase T1 (12.5 U) in a final volume of 5 μl containing 20 mM sodium citrate (pH 5), 6 M urea and 5 μg *E.coli* tRNA for 30 min at 30°C (25). For identification, RNA fragments were digested with RNase T1 (12.5 U) and RNase H (2 U) simultaneously in a total volume of 5 μl containing 50 mM Tris–HCl (pH 7.5) and 50 pmol specific oligodeoxynucleotide for 30 min at 37°C. The RNA fragments were analyzed on a denaturing 20% polyacrylamide gel as described above. The

following oligodeoxynucleotides (OSWEL DNA Service, Edinburgh) were used for site specific RNase H digestion:

oligo 18: 5′-CTT GAT ATT ATT TTT G-3′
oligo 21: 5′-CTA AGA AAG TGT AT-3′
oligo 31: 5′-GAA AAA ATG TTA GTA A-3′

RESULTS

PRP8 protein can be UV-crosslinked to pre-mRNA, IVS–exon 2 and IVS

Interactions of the yeast PRP8 protein with substrate RNA are splicing specific in that they are spliceosome assembly dependent and occur only with pre-mRNA capable of undergoing the first transesterification reaction (22). To identify the precursor-derived RNA species (pre-mRNA, intermediates and/or products) that interact with PRP8 protein, the following experiment was designed (Fig. 1): *In vitro* splicing reactions using uniformly [α-^{32}P]UTP labelled rp28 RNA or rp51A RNA as substrate were UV-irradiated at 254 nm to covalently crosslink protein–RNA contacts. Non-crosslinked, non-covalent interactions were then disrupted by denaturation and PRP8–RNA crosslinked complexes were immunoprecipitated by anti-PRP8 polyclonal antibodies. The immunoprecipitated RNA was recovered and identified on a denaturing 6% polyacrylamide gel. Since the different substrate RNA species are products of specific steps of the splicing reaction this experimental design allows the determination of the kinetics of PRP8–substrate–RNA interactions during splicing. For comparison, immunoprecipitation of intact spliceosomes with anti-PRP8 antibodies (by omitting the denaturation step) showed that under these conditions IVS, IVS–exon 2 and exon 1 were efficiently precipitated, whereas the spliced exons were very poorly precipitated, (22, data not shown). This is consistent with the observation that the spliced exons are rapidly released after the second transesterification reaction (26).

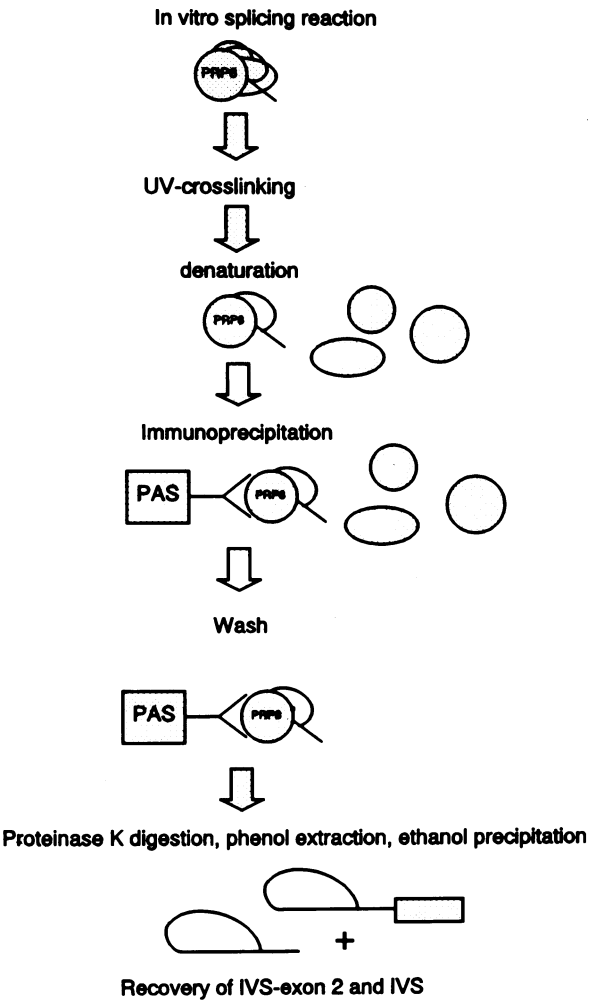

Figure 1. Strategy for identification of precursor-derived RNA species interacting directly with PRP8 protein during RNA splicing *in vitro*. Splicing reactions containing uniformly ^{32}P-labelled pre-mRNA were UV-irradiated, denatured and immunoprecipitated with PRP8-specific antibodies. The precipitated RNA was deproteinized, fractionated on a 6% denaturing polyacrylamide gel and analyzed by autoradiography (shown in Fig. 2).

Each of the following experiments was carried out separately with two different sets of anti-PRP8 antibodies, which produced identical results: polyclonal rabbit antibodies directed (i) to a synthetic peptide matching the N-terminus of PRP8 protein (anti-8.6) and (ii) to a β-galactosidase fusion protein with the C-terminus of PRP8 protein (anti 8.4). Following disruption of spliceosomes by denaturation, immunoprecipitation of PRP8 resulted in selective co-precipitation of the IVS and IVS–exon 2. Compared to the total reaction control, exon 1 and the spliced exons were not detectably precipitated (Fig. 2A, compare lanes 2 and 3). Analysis of the supernates of the immunoprecipitation reactions revealed large amounts of spliced exons and exon 1 (data not shown), indicating that the inability to precipitate these RNA species was not the result of degradation. Crosslinking of IVS or IVS–exon 2 to PRP8 protein was not observed in the absence of ATP, consistent with the previously observed dependence of the PRP8–RNA contact on ATP and spliceosome assembly (22). Control experiments using either preimmune serum or competition with the peptide to which the antibodies were raised ruled out the possibility of non-specific precipitation (Fig. 2A, lanes 5–7). Internal controls shown in Figure 2B (mixing of a UV-irradiated splicing reaction containing rp51 RNA with a non-irradiated splicing reaction containing rp28 RNA and *vice versa*, and then denaturation and precipitation as described above) confirmed that precipitation of IVS and IVS–exon 2 was dependent on crosslinking by UV-irradiation. In these and other control experiments a small amount of pre-mRNA was always non-specifically precipitated, therefore no conclusions could be drawn about interaction(s) of PRP8 protein with the unspliced precursor RNA.

A different approach was taken to investigate interactions of PRP8 protein with unspliced precursor RNA: splicing extract containing a temperature-sensitive mutant form of the PRP2 protein was heat-inactivated and then allowed to form spliceosomes upon the addition of ATP and uniformly ^{32}P-labelled pre-mRNA (PRP2Δ spliceosomes). Since PRP2 activity is an essential requirement for the first transesterification reaction (27) PRP2Δ spliceosomes could not process pre-mRNA into spliced mRNA (Fig. 3A, lanes 3–5), and they formed splicing complex I but no splicing complex II (28,29 and data not shown).

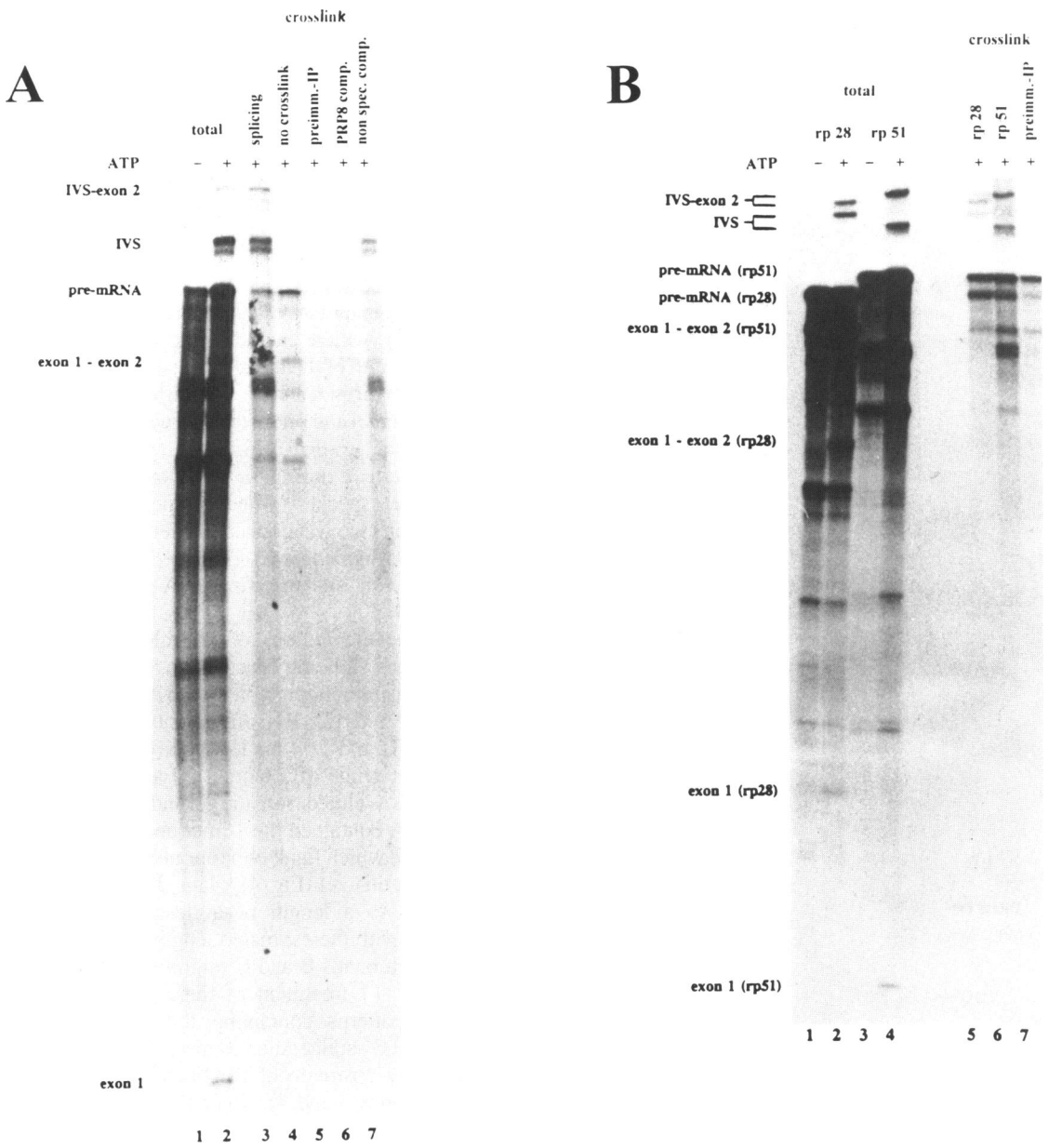

Figure 2. UV-crosslinking of precursor-derived RNA species to PRP8 protein. (**A**) *In vitro* splicing reactions (50 µl) containing uniformly ^{32}P-labelled rp51A pre-mRNA were irradiated with short wave UV-light, denatured and immunoprecipitated with 8.6 antibodies (lane 3). Negative controls were: no UV-irradiation (lane 4), immunoprecipitation with preimmune serum (lane 5), immunoprecipitation in the presence of the peptide to which the antibodies were raised (lane 6) or in the presence of a non-specific control peptide (lane 7). For comparison, total splicing reactions (0.2 µl) were incubated in the absence (lane 1) and presence (lane 2) of ATP. (**B**) UV-irradiated *in vitro* splicing reactions containing ATP and UV-crosslinked rp28 RNA were mixed with non-irradiated splicing reactions containing rp51A RNA (lane 5) and *vice versa* (lane 6) were denatured and immunoprecipitated with 8.6 antibodies. For preimmune-precipitation both rp28 RNA-containing samples and rp51 RNA-containing samples were UV irradiated and treated as described above (lane 7). For comparison, *in vitro* splicing reactions (0.2 µl) containing rp28 pre-mRNA (lanes 1 and 2) or rp51A pre-mRNA (lanes 3 and 4) were incubated in the absence (lanes 1 and 3) or presence (lanes 2 and 4) of ATP. RNA was fractionated on a 6% denaturing polyacrylamide gel. Positions of the pre-mRNA, the intervening sequence (IVS)–exon 2 intermediate, the free exon 1 intermediate and the IVS and exon 1–exon 2 products are indicated on the left.

Complementation with a heat-inactivated temperature-sensitive prp8 extract restored splicing activity (Fig. 3A, lanes 7–9).

Contacts of PRP8 protein in PRP2Δ spliceosomes were also investigated by UV-crosslinking experiments. Following UV-irradiation, samples were treated with RNase T1, immunoprecipitated by PRP8 specific antibodies, and proteins were separated by SDS–PAGE. Radiolabelling of PRP8 protein in PRP2Δ spliceosomes (Fig. 3B, lane 4) indicated a PRP8 protein–pre-mRNA interaction. Since UV-crosslinking of PRP8 protein in PRP2Δ spliceosomes complemented with a temperature-sensitive prp8 extract was no more efficient than in PRP2Δ spliceosomes alone (Fig. 3B, compare lanes 4 and 6), the observed interaction occurs before step 1 and was not due to residual splicing activity in the PRP2Δ extract.

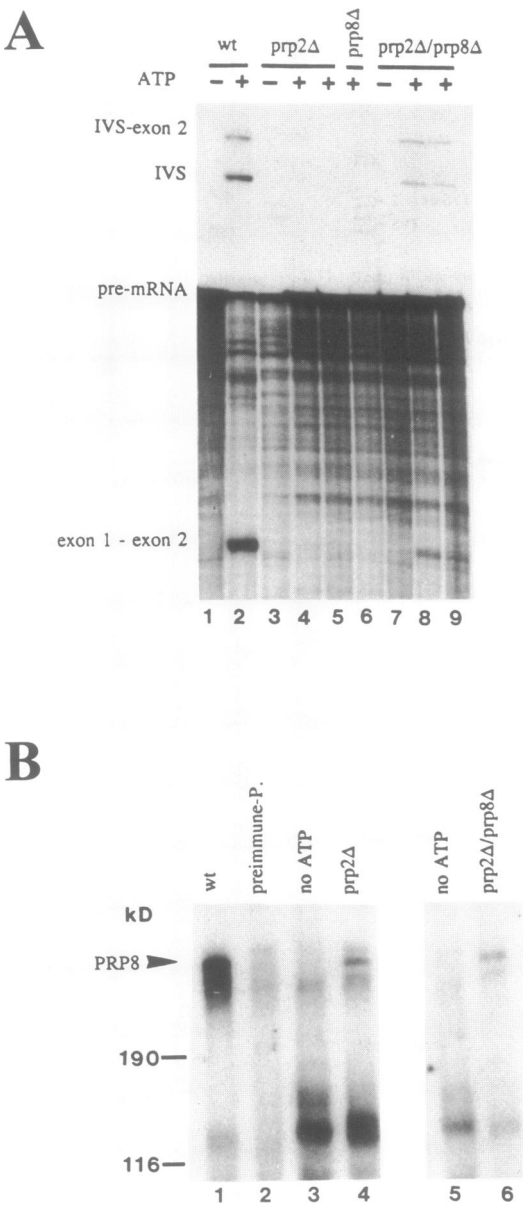

Figure 3. UV-crosslinking of PRP8 protein in PRP2Δ spliceosomes. (**A**) *In vitro* splicing reactions with uniformly ^{32}P-labelled rp28 RNA and splicing extract of a wild-type strain were incubated in the absence (lane 1) or presence (lane 2) of ATP; similarly, splicing activity was analyzed in reactions containing a temperature-sensitive extract from *prp2-1* cells after 15 min heat-inactivation at 31°C in the absence (lane 3) or presence (lane 4) of ATP, after 30 min heat-inactivation (lane 5) and in reactions containing a temperature-sensitive extract from *prp8.31* strain after 90 min heat-inactivation at 31°C (lane 6). Complementation of heat-inactivated extract from *prp8.31* cells with extract from *prp2-1* cells heat-inactivated for 15 min was monitored in the absence (lane 7) or presence (lane 8) of ATP and with prp2-1 extract heat-inactivated for 30 min (lane 9). RNA was fractionated on a 6% denaturing polyacrylamide gel. (**B**) *In vitro* splicing reactions were irradiated with short-wave UV light, digested with RNase T1 and subjected to immunoprecipitation with PRP8-specific antibodies. The immunoprecipitates were analyzed by SDS–PAGE followed by autoradiography to detect UV-crosslinked proteins. Immunoprecipitation of UV-crosslinked PRP8 protein using 8.6 antibodies is shown for splicing reactions containing ATP and wild-type splicing extract (lane 1), heat-inactivated prp2-1 extract (30 min at 31°C) precipitated with 8.6 preimmune-serum (lane 2) or with 8.6 antibodies in the absence (lane 3) and presence (lane 4) of ATP and complemented with heat-inactivated prp8.31 extract (90 min at 31°C) in the absence (lane 5) or presence (lane 6) of ATP. The migration of protein molecular weight markers is indicated on the left, as is the position of the PRP8 protein.

RNA fragments protected from ribonuclease T1 digestion and coprecipitated with anti-PRP8 antibodies include the 5′ splice site and the branchpoint-3′ splice site region

A ribonuclease T1 protection assay similar to that of Black *et al.* (30) was used to identify the regions of substrate RNA which were protected by yeast splicing complexes and immunoprecipitated with PRP8-specific antibodies. Rp28 substrate RNA was chosen for RNase T1 mapping because the digestion pattern produced fragments of unique length at the 5′ splice site (21 nucleotides exon sequence and 18 nucleotides intron sequence) and the branchpoint-3′ splice site region (a ladder of 25–29 nucleotides) which includes the polypyrimidine tract. The predicted length of the branchpoint-3′ splice site fragment was 31 nucleotides (Fig. 4A and B). The difference between the observed (Fig. 4C, lane 2) and predicted size was due to the presence of two long runs of uridines (Fig. 4A), which cause a 'nucleotide skipping' effect during *in vitro* transcription with T7 RNA polymerase, especially when uridine is limiting in the transcription reaction (see Materials and Methods). The identity of these pre-mRNA fragments was confirmed by targeting ribonuclease H digestion with site-specific DNA-oligonucleotides (data not shown).

To define the regions of pre-mRNA that are protected in spliceosomes, splicing reactions were treated with RNase T1, followed by immunoprecipitation with PRP8-specific antibodies. Three protected rp28 RNA fragments migrating at ~50 (band A), 70 (band B) and 200 nucleotides (band C) were co-immunoprecipitated (Fig. 4B, lane 3). Each of the three protected fragments was eluted from the gel and re-digested with RNase T1. Fragment A contained the 18mer and the 21mer adjacent to the 5′ splice site which flank two four nucleotide fragments too small to detect in this gel (Fig. 4D, lane 2). These fragments together correspond to a length of at least 47 nucleotides, in close agreement with the estimated length of 50 nucleotides for band A. Although bands B and C migrate differently on a denaturing gel, RNase T1 treatment of these bands resulted in identical digestion patterns containing the 5′ splice site 18mer, the branchpoint-3′ splice site '31mer' and a 9mer which mapped immediately upstream of the branchpoint consensus sequence (Fig. 4D, lanes 3 and 4). Since the '31mer' was found only in combination with the 18mer intron fragment, the aberrant migration of bands B and C could be due to a branched 'Y'-structure, resulting from protection of the branched region of the lariat.

DISCUSSION

A direct interaction of the yeast splicing factor PRP8 with the substrate RNA appears to be an important contribution to spliceosomal processing activity (22). A similar interaction of p220, the human homologue of the PRP8 protein, has been detected in the HeLa-splicing system (21). As a more detailed characterization of this interaction we report here that the yeast PRP8 protein interacts with the pre-mRNA, IVS–exon 2 and the IVS during the splicing process. Since the different RNA species are products of specific steps of the splicing reaction we conclude that the interaction of PRP8 protein with substrate RNA is established before step 1 of splicing (indicated by the crosslink to pre-mRNA in PRP2Δ spliceosomes) and is maintained during the splicing reaction (indicated by the crosslink to IVS–exon 2) until after completion of step 2 (indicated by the crosslink to excised

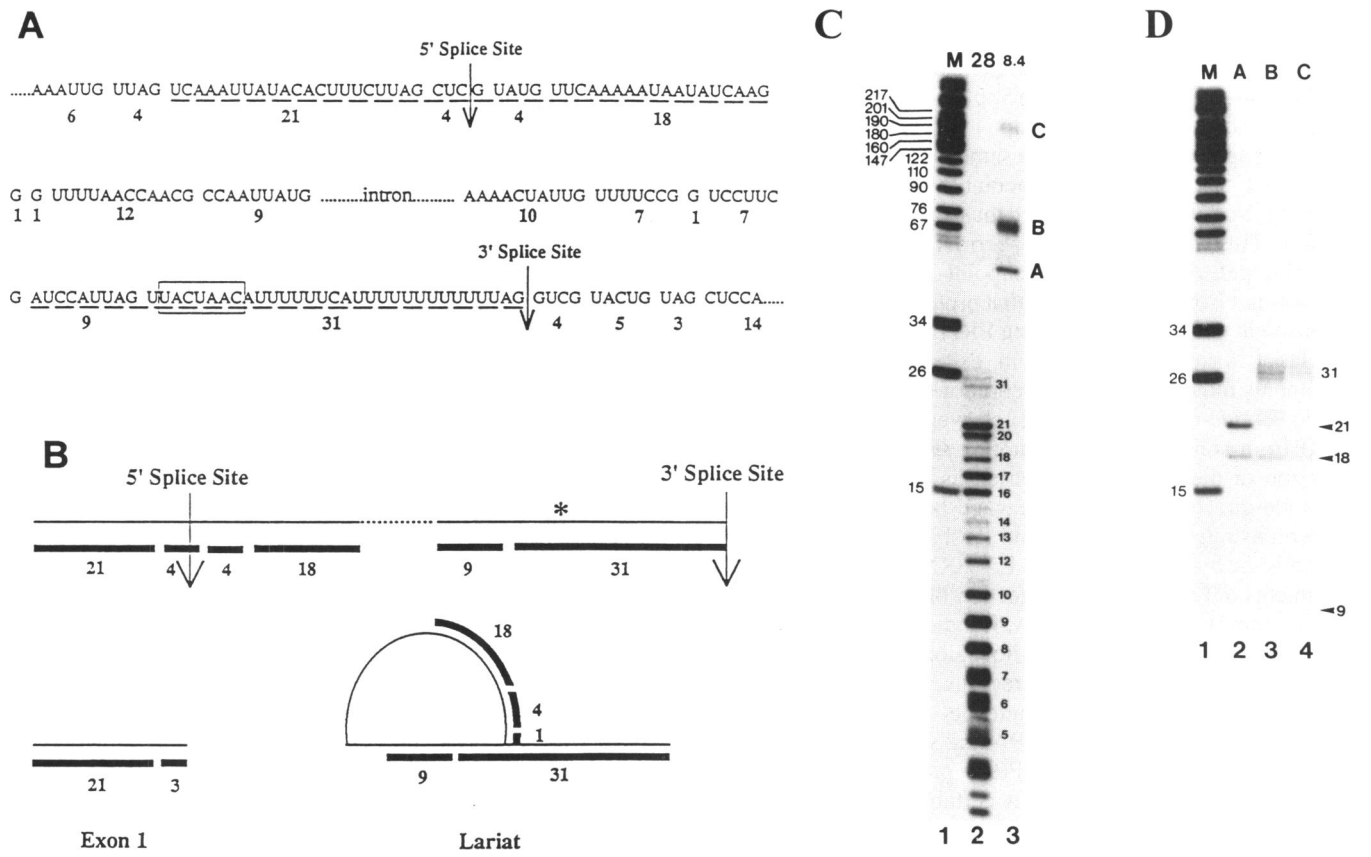

Figure 4. Analysis of rp28 RNA fragments protected from ribonuclease T1 digestion and precipitated from *in vitro* splicing reactions with PRP8 specific antibodies. (**A**) A partial nucleotide sequence of rp28 pre-mRNA, displayed according to the fragments generated by digestion with RNase T1. The numbers below the sequence refer to the nucleotide length of the individual digestion products. The regions of RNA protected by complexes immunoprecipitated with PRP8-specific antibodies are underscored with a broken line. 5′ and 3′ splice sites are indicated by vertical arrows, and the branchpoint consensus sequence UACUAAC is boxed. (**B**) The location of the protected oligoribonucleotides in rp28 pre-mRNA, splicing intermediates and excised intron. The pre-mRNA is shown as a thin line, with the site of branch formation indicated by an asterisk. 5′ and 3′ splice sites are represented by vertical arrows. The apparent length of the internal intron region of the pre-mRNA (dotted line) has been significantly shortened in this diagram. The locations of the protected oligoribonucleotides are shown as thick lines, with their nucleotide lengths indicated at each fragment. The oligoribonucleotides are positioned according to their location in the pre-mRNA molecule, exon 1 and the branch structure of the intron. (**C**) Uniformly ^{32}P-labelled rp28 pre-mRNA was incubated under splicing conditions and then digested with RNase T1; following immunoprecipitation with anti-8.4 antibodies RNA was fractionated on a 20% denaturing polyacrylamide gel; three RNA species A, B and C were detected (lane 3). Lane 1 shows a ^{32}P-end labelled *Msp*I-digested pBR322 DNA, with fragment sizes in nucleotides indicated on the left. The oligoribonucleotides generated by RNase T1 digestion of rp28 pre-mRNA (lane 2) have their respective nucleotide lengths indicated on the right. The 25–29 nucleotide ladder is labelled as '31' to indicate the full-length RNase T1 fragment from which it is derived. (**D**) Rp28 RNA fragments A, B and C were eluted from the gel shown in (C) and redigested with RNase T1. The oligoribonucleotides generated from digestion of the protected fragments A, B and C are shown in lanes 2, 3 and 4, respectively, with the nucleotide sizes of the oligoribonucleotides indicated on the right. The nucleotide size markers (M) in lane 1 are as described in (C).

IVS). The contact of PRP8 protein with the substrate RNA during the entire splicing process indicates that it most likely plays an important, probably even essential role in both transesterification reactions.

The crosslink to the IVS lariat demonstrates that PRP8 protein certainly interacts with intron nucleotides. However, interactions of PRP8 with both exons (in the pre-mRNA and the IVS–exon 2) cannot be excluded. Considering that the U5 snRNA has been shown to interact with exon nucleotides at both the 5′ and the 3′ splice sites in yeast and mammals (4–6 and A. Newman, personal communication) PRP8, being a U5 snRNP protein, might interact with these positions as well.

In fact, interaction of the human PRP8 homologue p220 with a modified 4-thio-uridine residue at the penultimate position of the 5′ exon has been demonstrated (31) and preliminary data suggest that the yeast PRP8 protein interacts with this position as well (S. T., A. J. Newman and J. D. B., unpublished data). In contrast to the inability to detect PRP8 crosslinking to free exon 1 in these experiments in which modified nucleotides were not used, UV-crosslinking of PRP8 protein to the photoactivatable uridine analogue 4-thioU in the 5′ exon could reflect the strongly enhanced crosslinking efficiency of 4-thio-uridine compared to normal uridine. Use of 4-thioU might allow the visualization of protein–RNA interactions which are not detectable by the much less efficient crosslinking with unmodified nucleotides.

Considering that PRP8 protein interacts with substrate RNA during the entire splicing process, it is particularly interesting to map the binding site(s) on the RNA. As a first step, substrate RNA fragments that were protected from RNase T1 digestion by spliceosomal complexes immunoprecipitated with PRP8-specific antibodies were identified by re-digestion with RNase T1, followed by annealing with specific DNA oligonucleotides

and RNase H digestion. The protection may be mediated by intact or partially disrupted spliceosomes containing PRP8 protein. One protected substrate RNA fragment included an exon 1 sequence and an intron sequence close to the 5 splice site, indicating that the protection occurred prior to step 1 of splicing. Two other protected fragments contained the same intron sequence close to the 5 splice site and the branchpoint-3′ splice site sequence, indicating branch formation and thus a 'Y'-structure of this fragment. This would explain the aberrant migration pattern on a denaturing gel. A protected branchpoint-3′ splice site sequence alone was not isolated, indicating that protection of this region by spliceosomal complexes containing PRP8 protein occurred only after lariat formation. This is in excellent agreement with experiments indicating that protection of the 3′ splice site from oligonucleotide-directed RNAse H cleavage requires the activity of PRP16, a splicing factor promoting step 2 of splicing (32). Protection of the branchpoint consensus sequence from oligonucleotide-directed RNase H cleavage before lariat formation was demonstrated by Rymond and Rosbash and is most likely accomplished by basepairing with U2 snRNA (33). Although our experiments did not allow the detection of direct interactions of PRP8 protein with substrate RNA, it indicates that the 5′ splice site and the branchpoint 3′ splice site region are potential binding sites for PRP8 protein. Other regions of intron and exons containing large RNase T1 fragments were not recovered, excluding the rest of the substrate RNA as strong binding sites for PRP8 protein. Considering that PRP8 protein could be cross-linked to IVS–exon 2 and IVS it certainly interacts with the branchpoint 3′ splice site region after the first transesterification reaction. These results provide an essential basis for interaction studies to precisely map the binding site(s) of PRP8 protein on the substrate RNA and the kinetics of these interaction(s).

Previous reports provide evidence that PRP8 protein could play a role in the protection and stability of RNAs and/or RNA–RNA interactions (20). A conserved nine nucleotide loop in U5 snRNA has been shown to interact with nucleotides of the 5′ and 3′ exons, allowing the U5 snRNA not only to hold free exon 1, but to align both exons for the second transesterification step (5,6). As PRP8 protein is a component of U5 snRNPs, it might be responsible for establishing and stabilising these U5 snRNA–pre-mRNA interactions. Confirmation of such a role for PRP8 will come from the precise mapping of the binding sites of PRP8 protein on the substrate RNA.

ACKNOWLEDGEMENTS

We are grateful to Andy Newman for critically reading the manuscript. Plasmid rp51A was kindly provided by Claudio Pikielny. This work was funded by the Cancer Research Campaign. EW was funded by a British Marshall Scholarship and the Cancer Research Campaign. JDB holds a Royal Society EPA Cephalosporin Fund Senior Research Fellowship.

REFERENCES

1 Rymond, B.C. and Rosbash, M. (1992). In Jones, E.W., Pringle, J.R. and Broach, J.R. (eds), *The Molecular and Cellular Biology of the Yeast Saccaromyces* (Vol. II), Cold Spring Harbor Laboratory Press, Cold Spring Harbor, NY, pp 143–192.
2 Moore, M.J., Query, C.C. and Sharp, P.A. (1993). In Gesteland, R.F., and Atkins, J.F. (eds), *The RNA World*, Cold Spring Harbor Laboratory Press, Cold Spring Harbor, NY, pp 303–357.
3 Madhani, H.D. and Guthrie, C. *Ann. Rev. Genet.* **28**, 1–26.
4 Newman, A.J. and Norman, C. (1991) *Cell* **65**, 115–123.
5 Sontheimer, E.J. and Steitz, J.A. (1993) *Science* **262**, 1989–1996.
6 Newman, A.J. and Norman, C. (1992) *Cell* **68**, 743–754.
7 Beggs, J.D. (1993) *Mol. Biol. Rep.* **18**, 99–103.
8 Krämer, A. (1993) *Mol. Biol. Rep.* **18**, 93–98.
9 Will, C.L., Behrens, S.-E. and Lührmann, R. (1993) *Mol. Biol. Rep.* **18**, 121–126.
10 Jackson, S.P., Lossky, M. and Beggs, J.D. (1988) *Mol. Cell Biol* **8**, 1067–1075.
11 Strauss, E.J. and Guthrie, C. (1991) *Genes Dev.* **5**, 629–641.
12 Jamieson, D.J., Rahe, B., Pringle, J. and Beggs, J.D. (1991) *Nature* **349**, 715–717.
13 Anderson, G.J., Bach, M., Lührmann, R. and Beggs, J.D. (1989) *Nature* **342**, 819–821.
14 Paterson, T., Beggs, J.D., Finnegan, D.J. and Lührmann, R. (1991) *Nucleic Acids Res.* **19**, 5877–5882.
15 Kulesza, H., Simpson, G.G., Waugh, R., Beggs, J.D. and Brown, J.W.S. (1993) *FEBS Lett.* **318**, 4–6.
16 Hodges, P.E., Jackson, S.P., Brown, J.D. and Beggs, J.D. (1995) *Yeast* **11**, in press.
17 Lossky, M., Anderson, G.J., Jackson, S.P. and Beggs, J.D. (1987) *Cell* **51**, 1019–1026.
18 Whittaker, E., Lossky, M. and Beggs, J.D. (1990) *Proc. Natl. Acad. Sci. USA* **87**, 2216–2219.
19 Pinto, A.L. and Steitz, J.A. (1989) *Proc. Natl. Acad. Sci. USA* **86**, 8742–8746.
20 Brown, J.D. and Beggs, J.D. (1992) *EMBO J.* **11**, 3721–3729.
21 Garcia-Blanco, M.A., Anderson, G.J., Beggs, J.D. and Sharp, P.A. (1990) *Proc. Natl. Acad. Sci. USA* **87**, 3082–3086.
22 Whittaker, E. and Beggs, J.D. (1991) *Nucleic Acids Res.* **19**,,5483–5489.
23 Pikielny, C.W. and Rosbash, M. (1986) *Cell* **45**, 869–877.
24 Lin, R.-J., Newman, A.J., Cheng, S.-C. and Abelson, J. (1985) *J. Biol. Chem.* **260**, 14780–14792.
25 Donis Keller, H., Maxam, A.M. and Gilbert, W. (1977) *Nucleic Acids Res.* **4**, 2527–2538.
26 Company, M., Arenas, J. and Abelson, J. (1991) *Nature* **349**, 487–493.
27 Lin, R.-J., Lustig, A.J. and Abelson, J. (1987) *Genes Dev.* **1**, 7–18.
28 King, D.S. and Beggs, J.D. (1990) *Nucleic Acids Res.* **18**, 6559–6564.
29 Teigelkamp, S., McGarvey, M., Plumpton, M. and Beggs, J.D. (1994) *EMBO J.* **13**, 888–897.
30 Black, D.L., Chabot, B. and Steitz, J.A. (1985) *Cell* **42**, 737–750.
31 Wyatt, J.R., Sontheimer, E.J. and Steitz, J.A. (1992) *Genes Dev.* **6**, 2542–2553.
32 Schwer, B. and Guthrie, C. (1992) *EMBO J.* **11**, 5033–5039.
33 Rymond, B.C. and Rosbash, M. (1986) *EMBO J.* **5**, 3517–3523.